Acta Pharmacologica Sinica

www.nature.com/aps

ARTICLE

Adriamycin induces cardiac fibrosis in mice via PRMT5-mediated cardiac fibroblast activation

Xiao-liang Dong[1], Bao-hui Yuan[2,3], Sheng-zhou Yu[1], He Liu[2,3], Xiao-hua Pan[2,3], Jia Sun[2,3] and Li-long Pan[1]

Long-term treatment with adriamycin (ADR) is associated with higher incidences of cumulative cardiotoxicity manifest as heart failure. ADR-induced cardiomyopathy is characterized by extensive fibrosis that is caused by cardiac fibroblast activation. To date, however, no specific treatment is available to alleviate ADR-induced cardiotoxicity. Protein arginine methyltransferase 5 (PRMT5), a major enzyme responsible for methylation of arginine, regulates numerous cellular processes such as cell differentiation. In the present study we investigated the role of PRMT5 in cardiac fibrosis. Mice were administered ADR (3 mg/kg, i.p., every 2 days) for 2 weeks. We showed that aberrant PRMT5 expression was largely co-localized with α-SMA-positive activated cardiac fibroblasts in ADR-injected mice and in ADR-treated cardiac fibroblasts in vitro. PRMT5-overexpression exacerbated, whereas PRMT5 knockdown alleviated ADR-induced cardiac fibrosis in vivo and TGF-β1-induced cardiac fibroblast activation in vitro. We demonstrated that PRMT5-overexpression enhanced methylated-Smad3 levels in vivo and in vitro. Pretreatment with a specific PRMT5 inhibitor EPZ015666 (5 nM) or overexpression of a catalytically inactive mutant of PRMT5, PRMT5(E444Q), reduced PRMT5-induced methylation of Smad3, thus suppressing PRMT5-mediated cardiac fibroblast activation in vitro. Furthermore, ADR activated cardiac fibroblasts was depending on autocrine TGF-β1. Taken together, our results demonstrate that PRMT5 promotes ADR-induced cardiac fibrosis via activating cardiac fibroblasts, suggesting that it may be a potential therapeutic target of ADR-caused cardiotoxicity.

Keywords: adriamycin; cardiotoxicity; cardiac fibrosis; cardiac fibroblasts; protein arginine methyltransferase 5; transforming growth factor-β1

Acta Pharmacologica Sinica (2023) 44:573–583; https://doi.org/10.1038/s41401-022-00963-x

INTRODUCTION

Adriamycin (ADR), an efficacious antineoplastic agent, is widely used to treat both solid tumors and hematological malignancies [1–3]. Despite its extensive use and potential clinical usefulness, long-term therapy with ADR is associated with higher incidences of cumulative cardiotoxicity manifest as heart failure [4–6]. Histologically, ADR-induced cardiomyopathy is characterized by extensive fibrosis [7]. Activated fibroblasts are the fundamental cellular effectors of cardiac fibrosis, serving as the main ECM-producing cells. Conversion of fibroblasts into secretory, matrix-producing and contractile cells, called myofibroblasts, is a crucial cellular event in cardiac fibrosis [8]. To date, no specific treatment can be unanimously recommended for alleviating ADR-induced cardiotoxicity [9]. Poor prognosis and high mortality rates are still inevitable. Accordingly, there is an urgent need to further study the mechanism of ADR-induced cardiotoxicity and develop new strategies to prevent or treat ADR-related cardiovascular complications.

Arginine methylation is a posttranslational modification of histones and other proteins that has regulatory effects on physiological processes, including cell proliferation, differentiation, and development [10–12]. Protein arginine methyltransferase 5 (PRMT5), a class-II protein arginine methyltransferase, is involved in a wide range of biological processes. PRMT5 mediates symmetric dimethylation of the third arginine residue of histone 4 (H4R3) and H3R8 [13]. Previous studies suggested that PRMT5 is an oncogene that promotes the process of cancer cell proliferation, migration, and invasion [14]. PRMT5 is also identified as a critical epigenetic regulator in differentiation of many cell types, including oligodendrocyte differentiation [15], osteogenic differentiation [16] and chondrocyte differentiation [17]. Nevertheless, whether PRMT5 regulates the activation and differentiation of fibroblasts during cardiac fibrosis remains poorly recognized and understood.

In this study, we demonstrate that PRMT5 enhances mothers against decapentaplegic homolog 3 (Smad3) activation through methylation modification, which leads to activation of TGF-β1-Smad3 signaling, and ultimately promoting the differentiation and migration of cardiac fibroblasts and ADR-induced cardiac fibrosis. Our study provides novel evidence that PRMT5 critically mediates ADR-mediated cardiac fibrosis via Smad3 methylation.

MATERIALS AND METHODS

Reagents and antibodies

The ADR (MB1087) was purchased from meilunbio (Dalian, Liaoning, China). SB525334 (S1476) was obtained from Selleck Chemicals (Shanghai, China). (E)-SIS3 (HY-13013) was purchased from MedChemExpress (Shanghai, China). Anti-α-smooth muscle

[1]Wuxi School of Medicine, Jiangnan University, Wuxi 214122, China; [2]School of Food Science and Technology, Jiangnan University, Wuxi 214122, China and [3]State Key Laboratory of Food Science and Technology, Jiangnan University, Wuxi 214122, China
Correspondence: Jia Sun (jiasun@jiangnan.edu.cn) or Li-long Pan (llpan@jiangnan.edu.cn)
These authors contributed equally: Xiao-liang Dong, Bao-hui Yuan

Received: 20 March 2022 Accepted: 21 July 2022
Published online: 2 September 2022

actin (α-SMA) (ab124964), anti-fibronectin (ab45688), anti-connective tissue growth factor (CTGF) (ab6992), anti-Smad3 (phosphor S423 + S425) (ab52903) and anti-Smad3 (ab40854) antibodies were purchased from Abcam technology (Cambridge, UK). Anti-TGF-β1 (A15103), anti-pan-Symmetric-Di-Methyl Arginine (A18261) antibodies were obtained from ABclonal Technology (Wuhan, Hubei, China). Anti-PRMT5 (sc-376937), anti-collagen I (sc-59772) antibodies were purchased from Santa Cruz Biotechnology (Shanghai, China). Anti-α-smooth muscle actin (α-SMA) (#19245) was obtained from Cell Signaling Technology (Shanghai, China). Anti-glyceraldehyde-3-phosphate dehydrogenase (GAPDH) (AP0063), Goat anti-Rabbit IgG (H&L)-horseradish peroxidase (HRP) (BS13278), and Goat anti-Mouse IgG (H&L)-HRP (BS12478) antibodies were obtained from Bioworld Technology (Nanjing, Jiangsu, China). Anti-Flag (20543-1-AP) were purchased from Proteintech (Rosemont, IL, USA).

Plasmids and lentivirus production

pLVX-U6-EGFP (pGLV1-1)-PRMT5, the packaging plasmid psPAX2, and the envelope plasmid pMD2.G were kept in our laboratory. pLVX-U6-EGFP (pGLV1-1)-scramble-shRNA and pLVX-U6-EGFP (pGLV1-1)-PRMT5-shRNA (target sequence: 5′-GCACAGTTTGA GATGCCTTAT-3′) were obtained from GenePharma Co., Ltd (Shanghai, China). The plasmids pcDNA3.1/Flag-PRMT5(WT), pcDNA3.1/Flag-PRMT5(E444Q) (glutamine replaced glutamic acid in the 444th amino terminal position) were purchased from GENEWIZ (Suzhou, Jiangsu, China). All plasmids were verified by sequencing in Sangon Biotech (Shanghai, China) and purified using the Endofree Plasmid Preparation kit (12391, Qiagen, Hilden, Germany).

The lentivirus production was performed as previously described [18]. Briefly, HEK293T cells were co-transfected with the pLVX-U6-EGFP (pGLV1-1)-PRMT5-shRNA, the packaging plasmid psPAX2, and the envelope plasmid pMD2.G (at a mass ratio of 4: 3: 1) using Lipofectamine™ 3000 system (L3000008, Invitrogen, CA, USA) according to the manufacturer's instructions. After 72 h transfection, cell supernatants containing the lentivirus were collected, filtered with 0.45 μm filters, and concentrated through ultracentrifugation at 100,000 × *g* for 2 h. Viral titers were measured by QuickTiter™ Lentivirus Titer Kit (VPK-112, Cell Biolabs, CA, USA). Viruses were stocked at −80 °C for further use.

In vivo delivery of lentivirus and ADR administration

C57BL/6 male mice, aged 6–8 weeks, were purchased from JOINN Laboratories (Suzhou, Jiangsu, China). Mice were raised under conventional controlled conditions (22 °C, 55% humidity and day–night cycle) and had free access to a standard diet and tap water. All mice were allowed to acclimate to these conditions for at least 2 days before inclusion in experiments. All animal experimental procedures were approved by the Jiangnan University Experimental Animal Management and Animal Welfare Ethics Committee (IACUC Issue Number: JN. No 20190930c0501210). In vivo lentivirus delivery was conducted as previously described [19]. In brief, mice were anaesthetized with pentobarbital sodium (50 mg/kg) by an intraperitoneal injection, orally intubated, and connected to a rodent ventilator (R405, RWD Life Science Co.,LTD). An amount of lentivirus (with a titer of 10^7 TU/mL) containing PRMT5-shRNA or scramble-shRNA plasmids (30 μL) was intramyocardially injected with a 32 G needle into the left ventricle in approximately three sites. ADR was administered intraperitoneally every 2 days (3 mg/kg) for 2 weeks. Controls were administered saline intraperitoneally at the same volume.

Cardiac fibroblasts isolation, culture, and transfection

Neonatal ventricular fibroblasts were isolated and digested by trypsin and collagenase from the hearts of C57BL/6 mice as previously reported [20]. Briefly, the collected hearts were minced and digested with a collagenase I (1 mg/mL) and trypsin (1 mg/mL) solution (a ratio of 2:1). After eight digestions, the pellet was filtered and pre-plated for 1.5 h at 37 °C under 5% CO_2 to separate cardiac fibroblasts from cardiomyocytes. Cardiac fibroblasts in passage 0 were kept in culture for a maximum of 1 week or before attaining confluence prior to plating for experiments (passage 1), in order to dodge differentiation into myofibroblasts. Fibroblasts were cultured in Dulbecco's Modified Eagle's Medium (DMEM) supplemented with 10% fetal bovine serum for three generations. Cell transfection was administered according to our previous study [21]. Briefly, cardiac fibroblasts were seeded into 12-well plates 24 h before transfection at a confluence of 80%. Transient transfection was executed using Lipofectamine™ 3000 system according to the manufacturer's instructions. Briefly, Lipofectamine™ 3000 was added to Opti-MEM™ Medium (31985-070, Gibco, Shanghai, China) along with plasmid DNA and P3000 reagent and incubated for 15 min. Lastly, DNA–lipid complex was added to cells. In all cases, the total amount of DNA was normalized by the addition of control plasmids.

Histochemical analyses

After the animal model was completed, the whole heart was collected and fixed with 4% paraformaldehyde for 24 h. The tissues were dehydrated and paraffin-embedded, and the paraffin sections were prepared into 4 μm thick paraffin sections. The deposition of collagen in the myocardium of mice was detected by Masson trichrome staining. According to the protocol of Masson trichrome staining kit (BP-DL021, Sbjbio life Science, Nanjing, Jiangsu, China), the sections were dewaxed and stained with Weigert ferrixylin for 5–10 min, then they were differentiated with acidic ethanol differentiation solution and washed with water. Followingly, the sections were stained with Ponceau S- acid fuchsin solution for 5–10 min. After being treated with 1% glacial acetic acid for 1 min, the sections were washed with phosphomolybdic acid solution for 1–2 min. Sections were then restained with 2% aniline blue solution for 2 min. The sections were dehydrated with 95% ethanol for several times and then dehydrated with anhydrous ethanol. The sections were transparent with xylene and sealed with neutral resin for further detection and analysis.

Immunofluorescence

For cardiac tissue, the sections were dewaxed, followed by antigen-repairing with 0.01 mol/L sodium citrate at pH 6.0 (P0083, Beyotime Biotechnology, Shanghai, China). For cardiac fibroblasts, the slides were fixed with 4% paraformaldehyde (P0099, Beyotime), followed by permeating with 0.5% triton X-100 (P0096, Beyotime). Then, the tissues and cells were incubated at room temperature (RT) with 10% donkey serum for 1 h, and the diluted primary antibody (α-SMA: 1:200; PRMT5: 1:200) was added for overnight incubation. The next day, secondary antibody was added and incubated at RT for 1 h. Finally, the tissues and cardiac fibroblasts were examined using the Carl Zeiss LSM880 confocal laser microscope system (Tokyo, Japan) after 4′,6-diamidino-2-phenylindole staining.

Western blot

Tissues and cells were lysed by using lysis buffer (P0013, Beyotime) and centrifuged at 13,000 × *g*/min, 4 °C. The supernatant was collected and the protein concentration was determined using bicinchoninic acid protein assay kit (MA0082, Meilunbio, Dalian, Liaoning, China). Then the protein samples incubated with a sodium dodecyl sulfate (SDS) sample loading buffer were heated in the boiling water bath for 10 min, then subjected to 12% SDS-polyacrylamide gel (PAGE), and transferred onto polyvinylidene fluoride membranes. After blocked in 5% fat-free milk at RT for 1 h, membranes were incubated overnight at 4 °C with primary antibodies, followed by HRP-conjugated secondary antibodies for 1 h at RT. Finally, membrane-bound antibodies were detected by using a chemiluminescence reagent. The total protein content of loading was monitored by reprobing the same blots with loading control.

Quantitative real-time PCR (qRT-PCR)

Total RNA was isolated using TRIzol reagent (Life Technologies, MA, USA) and was subjected to reverse transcription using Prime-Script RT reagent kit (TaKaRa Biotechnology, Kyoto, Japan) following the manufacturer's instructions. SYBR® Green qRT-PCR was performed using qRT-PCR system (BIO RAD CFX Connect, CA, USA). The relative mRNA levels were normalized to mRNA levels of *β-actin* (housekeeping control), and calculations for fold change of each mRNA were made on comparative cycle threshold method ($2^{-\Delta\Delta Ct}$). The primers used in this study were provided in Supplementary Table S1.

Wound healing assay

The wound healing assay was conducted as previously reported [22]. Cardiac fibroblasts were allowed to be grown to 80%–90% confluence and then planted in 12-well plates. Scratches were documented under a microscope with ×10 magnification (Ti-U, Nikon, Japan) immediately after a scratch made by a 200 μL pipette tip at 0 h and once more when kept at 37 °C and 5% CO_2 for 20–24 h. Pictures were taken exactly at the same position before and after the incubation to document artificial wound closure. Wound area was calculated using ImageJ software (version 1.8.0_172). The wound sizes at different time points were expressed as percentages of the wound area on day 0.

Transwell assay

The transwell assay was conducted using a transwell chamber (8 μm pores, Corning Star, Cambridge, Mass, USA) as previously reported [23]. Briefly, cardiac fibroblasts were suspended with 200 μL of serum-free DMEM and seeded into the top chamber, while the bottom chamber contained DMEM with 20% FBS and indicated stimulants. Cells located on the upper surfaces of the transwell chambers were removed 24 h later. Cells migrated were fixed with 4% paraformaldehyde (P0099, Beyotime) followed by staining with 0.1% crystal violet (C0121, Beyotime). The stained cells were then photographed and counted under an upright microscope (80i, Nikon, Japan). Cells were quantified as the average number of cells found in five random microscopic fields. Three repeated experiments were carried out.

Data and statistical analysis

All statistical analyses were carried out by using GraphPad Prism software (version 8.2.1.441; GraphPad Software Inc., San Francisco, CA, USA). Error bars for in vitro and in vivo analysis represent the standard error of mean among intra-class data collected from independent experiments. The group size for statistical analysis was $n = 6$. The distribution of the data was tested with the Shapiro–Wilk normality test. For comparing the difference between two groups, a two-tailed, unpaired Student's t test was used. Comparisons between groups were analyzed using a one-way ANOVA followed by a Tukey's post hoc test. Post hoc tests were run only if F achieved $P < 0.05$ and there was no significant variance inhomogeneity. A value of $P < 0.05$ was considered statistically significant.

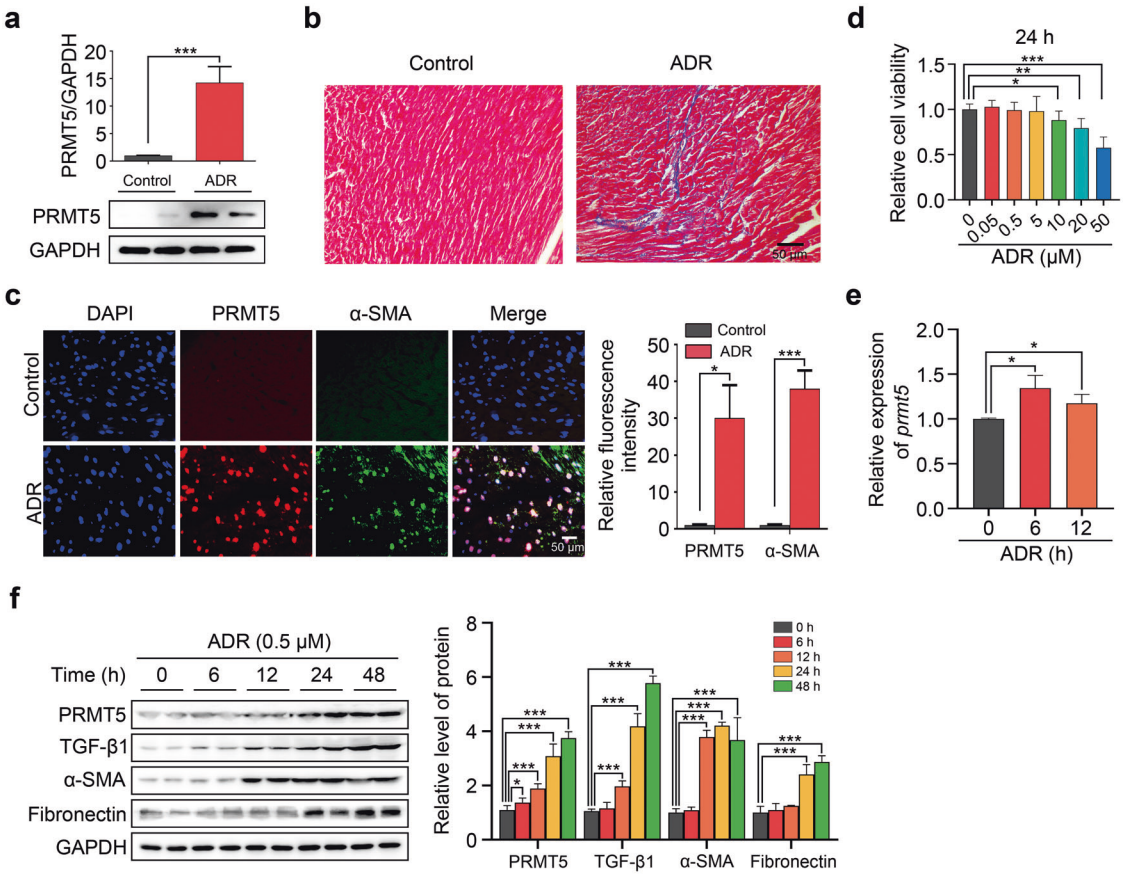

Fig. 1 PRMT5 is overexpressed in ADR-induced cardiac fibrosis in vivo and cardiac fibroblasts activation in vitro. a Mice were treated with ADR, and the abundance of PRMT5 in cardiac tissues was detected using Western blot. **b** Mice were treated with ADR and collagen deposition in the myocardium of mice was detected by Masson staining. **c** Immunofluorescence was applied to detect the expression of PRMT5 and α-SMA in the cardiac tissue obtained from ADR-treated mice. **d** Fibroblasts were treated with different concentrations of ADR for 24 h, and cell viabilities were detected by MTT assay. **e** Fibroblasts were treated with ADR (0.5 μM) for 6 and 24 h, and expression of *prmt5* was detected by RT-qPCR. **f** Fibroblasts were treated with ADR (0.5 μM) for indicated time, and then the cell lysates were applied to Western blot assay with indicated antibodies. Data of at least three independent experiments are presented as mean ± SEM, $n = 6$, *$P < 0.05$; **$P < 0.01$; ***$P < 0.001$, compared with control.

RESULTS

PRMT5 is upregulated in ADR-induced cardiac fibrosis in vivo and cardiac fibroblasts activation in vitro

Cardiac PRMT5 expression was considerably upregulated in mice with ADR-mediated cardiotoxicity, accompanied by the enhanced collagen deposition in cardiac tissue (Fig. 1a, b). Interestingly, aberrant PRMT5 expression was found predominantly co-localized with α-SMA-positive activated cardiac fibroblasts (Fig. 1c). As activated fibroblasts are the fundamental cellular effectors of cardiac fibrosis [24], we next investigated whether ADR treatment affected PRMT5 expression in cardiac fibroblasts in vitro. Firstly, cytotoxic effect of ADR on cardiac fibroblasts was observed when the concentration was greater than 0.5 μM (Figs. 1d, S1a, b). ADR at 0.5 μM markedly enhanced *prmt5* mRNA level and time-dependently upregulated PRMT5 protein expression in cardiac fibroblasts (Fig. 1e, f). Concomitantly, ADR time-dependently activated cardiac fibroblasts, evidenced by enhanced expression of TGF-β1, α-SMA and fibronectin (Fig. 1f). All these data indicate that PRMT5 is related to ADR-induced cardiac fibrosis and cardiac fibroblasts activation.

PRMT5 promotes cardiac fibrosis in vivo

Subsequently, we investigated whether overexpressed PRMT5 regulated cardiac fibrosis in vivo. Knockdown of PRMT5 by lentiviral shRNA attenuated ADR-induced cardiac fibrosis (Figs. 2a, S2), evidenced by reduced abundance of TGF-β1, α-SMA, fibronectin, collagen I, CTGF, MMP9 and decreased collagen deposition in cardiac tissues (Fig. 2b, c). Conversely, overexpression of PRMT5 significantly enhanced ADR-induced expression of TGF-β1, α-SMA, fibronectin, CTGF, MMP9, and collagen deposition in cardiac tissues (Fig. 2d, e). All these data indicate that aberrant PRMT5 expression promotes ADR-induced cardiac fibrosis in vivo.

PRMT5 promotes the activation of cardiac fibroblasts in vitro

Followingly, we investigated whether overexpressed PRMT5 regulated activation of cardiac fibroblasts, as shown in Fig. 3a, knockdown of PRMT5 significantly inhibited TGF-β1-mediated cardiac fibroblasts activation, as evidenced by the reduced expression of α-SMA, fibronectin and collagen I. Moreover, knockdown of PRMT5 significantly reduced TGF-β1-dependent

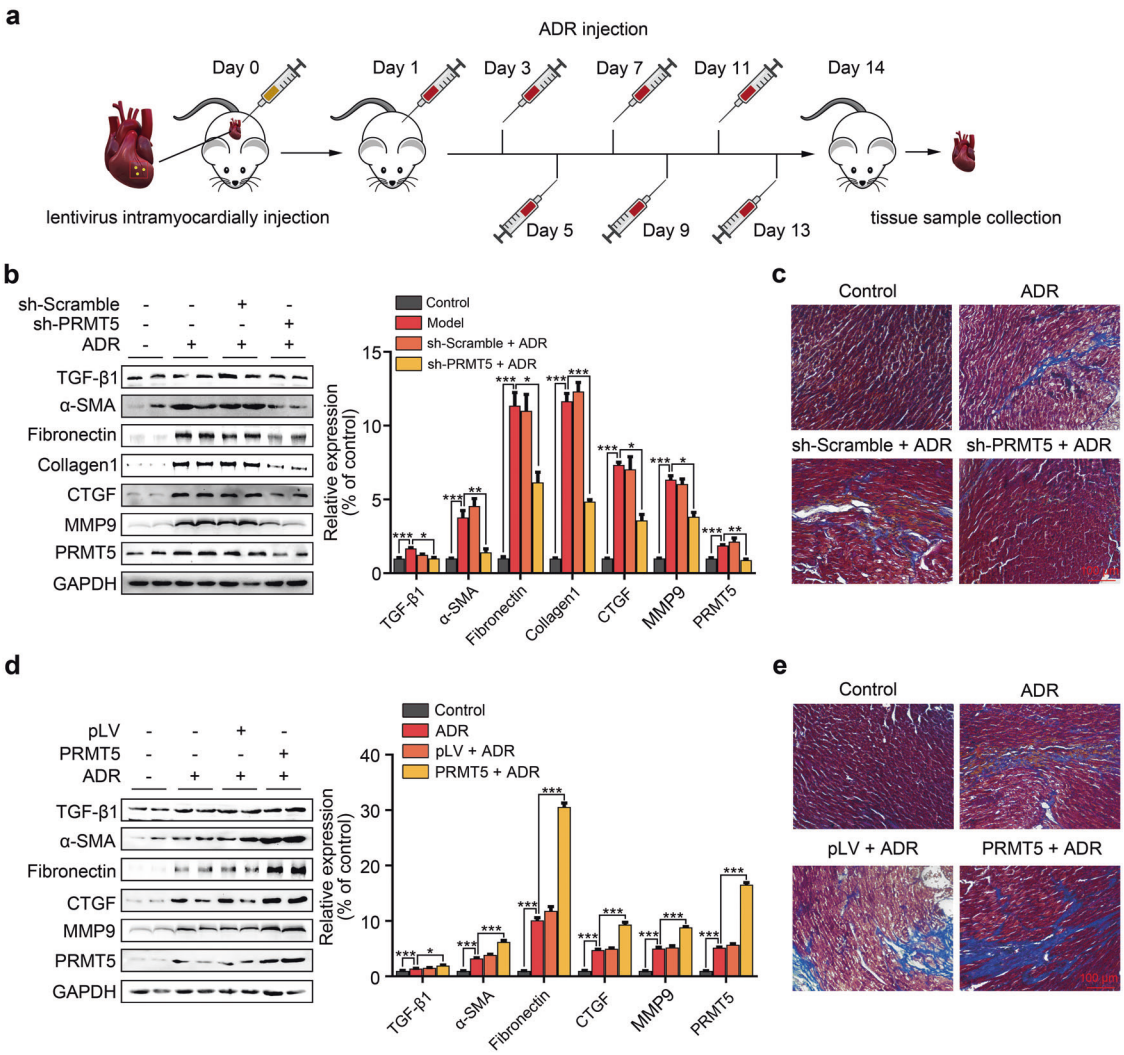

Fig. 2 PRMT5 promotes cardiac fibrosis in vivo. **a** Diagram of mice fibrosis model establishment. **b** Mice were transfected with PRMT5-shRNA plasmids and then treated with ADR, the cardiac tissues were obtained and then subjected into immunoblotting with indicated antibodies. **c** Mice transfected with PRMT5-shRNA plasmids were treated with ADR, the collagen deposition in the myocardium was detected by Masson staining. **d** Mice were transfected with PRMT5-shRNA plasmids and then treated with ADR, the cardiac tissues were obtained and then subjected into immunoblotting with indicated antibodies. **e** Mice transfected with PRMT5 plasmids were treated with ADR and, the collagen deposition in the myocardium was detected by Masson staining. Data of at least three independent experiments are presented as mean ± SEM, $n = 5$, $^{*}P < 0.05$; $^{**}P < 0.01$; $^{***}P < 0.001$, compared with control.

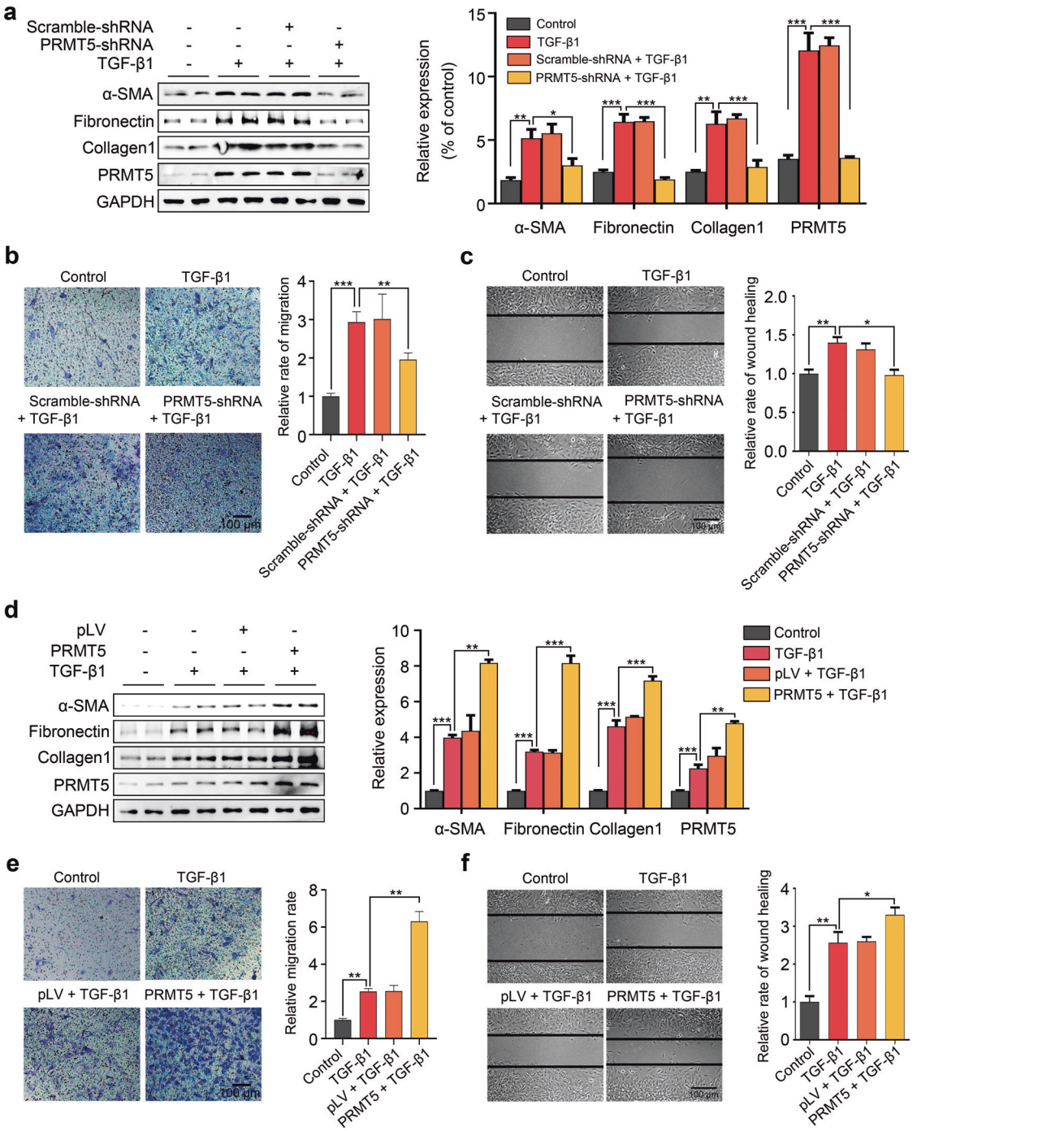

Fig. 3 PRMT5 promotes the activation of cardiac fibroblasts in vitro. a Cardiac fibroblasts transfected with Scramble-shRNA (2 μg/mL) or PRMT5-shRNA (2 μg/mL) plasmids were treated with TGF-β1 (5 ng/mL) for 24 h followed by immunoblotting with indicated antibodies. **b**, **c** Cardiac fibroblasts transfected with Scramble-shRNA (2 μg/mL) or PRMT5-shRNA (2 μg/mL) plasmids were treated with TGF-β1 (5 ng/mL) for 24 h. Migration of cardiac fibroblasts was detected using transwell assay (**b**) and wound healing assay (**c**). **d** Cardiac fibroblasts transfected with pLV (2 μg/mL) or PRMT5 (2 μg/mL) plasmids were treated with TGF-β1 (5 ng/mL) for 24 h followed by immunoblotting with indicated antibodies. **e**, **f** Cardiac fibroblasts transfected with pLV (2 μg/mL) or PRMT5 (2 μg/mL) plasmids were treated with TGF-β1 (5 ng/mL) for 24 h. Migration of cardiac fibroblasts was detected using transwell assay (**e**) and wound healing assay (**f**). Data of at least three independent experiments are presented as mean ± SEM, $n = 6$, $^{*}P < 0.05$; $^{**}P < 0.01$; $^{***}P < 0.001$, compared with control.

cardiac fibroblast migration (Fig. 3b, c). Conversely, overexpression of PRMT5 further enhanced TGF-β1-induced expression of α-SMA, fibronectin and collagen I (Fig. 3d). Meanwhile, overexpression of PRMT5 promoted TGF-β1-induced cardiac fibroblast migration (Fig. 3e, f). These data support that PRMT5 promotes the activation of cardiac fibroblasts in vitro.

PRMT5 promotes activation of Smad3 signaling in vivo and in vitro

TGF-Smad3 signaling plays a critical role in cardiac fibroblast activation and cardiac fibrosis [25]. We subsequently investigated the signaling mechanism of PRMT5 in coordinating the activation of Smad3 during ADR-induced cardiac fibrosis and in TGF-β1-treated cardiac fibroblasts. Knockdown of PRMT5 notably

inhibited Smad3 phosphorylation during ADR-induced cardiac fibrosis in vivo, while overexpression of PRMT5 significantly enhanced the phosphorylation of Smad3 (Fig. 4a, b). Consistent with the results in vivo, downregulation of PRMT5 also inhibited TGF-β1-elevated phosphor-Smad3 (p-Smad3) in cardiac fibroblasts (Fig. 4c). Conversely, PRMT5 overexpression evidently enhanced

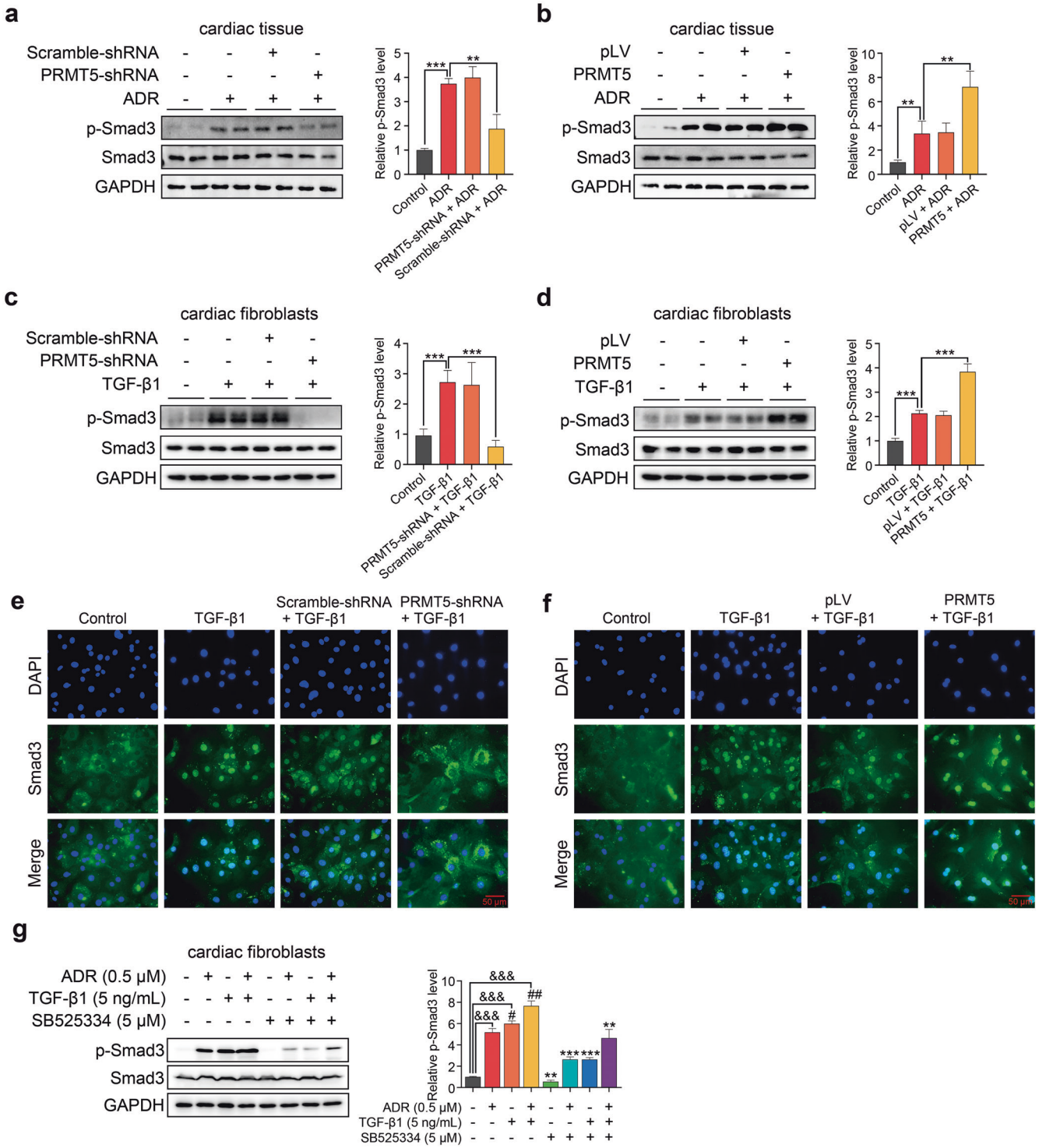

Fig. 4 PRMT5 strengthens activation of Smad3 during ADR-induced cardiac fibrosis and TGF-β1-treated cardiac fibroblasts. a, **b** Mice were transfected with PRMT5-shRNA (**a**) or PRMT5 overexpression (**b**) plasmids and then were treated with ADR, cardiac tissues were obtained and subjected into immunoblotting with indicated antibodies. **c**, **d** Cardiac fibroblasts transfected with PRMT5-shRNA (**c**) or overexpression (**d**) plasmids were treated with TGF-β1 (5 ng/mL) for 24 h followed by immunoblotting with indicated antibodies. **e**, **f** Cardiac fibroblasts transfected with PRMT5-shRNA (**e**) or overexpression (**f**) plasmids were treated with TGF-β1 (5 ng/mL) for 6 h, Smad3 nuclear translocation was detected by immunofluorescence. **g** Cardiac fibroblasts pre-incubated with SB525334 for 2 h were treated with ADR or TGF-β1 for 24 h, and then the cell lysates were subjected into immunoblotting with indicated antibodies. Data of at least three independent experiments are presented as mean ± SEM, $n = 5$, $^{**}P < 0.01$; $^{***}P < 0.001$, compared with control; $^{\#}P < 0.05$; $^{\#\#}P < 0.01$, compared with ADR-treated group; $^{\&\&\&}P < 0.001$ compared with the non-treated group.

TGF-β1-elevated p-Smad3 in cardiac fibroblasts (Fig. 4d). Consistent with the Western blot results, downregulation of PRMT5 inhibited the nuclear translocation of Smad3 while overexpression of PRMT5 promoted it (Fig. 4e, f). In addition, a TGF-β receptor I inhibitor, SB525334, blocked ADR- or TGF-β1-induced Smad3 phosphorylation (Fig. 4g). These results indicate that PRMT5 promotes Smad3 activation during ADR-induced cardiac fibrosis and in TGF-β1-treated cardiac fibroblasts.

PRMT5 promotes Smad3 phosphorylation to activate cardiac fibroblast *via* methylation modification

Subsequently, we investigated the molecular mechanism of PRMT5-mediated Smad3 activation. PRMT5 acts primarily through its methyltransferase activity, and it has been reported that methylation can promote phosphorylation [26]. As shown in Fig. 5a, TGF-β1-induced Smad3 methylation, which was further enhanced by PRMT5 overexpression. In contrast, treatment with a PRMT5 inhibitor EPZ015666 markedly inhibited both levels of p-Smad3 and methylated-Smad3 (me-Smad3) in TGF-β1-stimulated cardiac fibroblasts (Fig. 5b). In addition, we transfected plasmids expressing constitutively inactive mutant of PRMT5, PRMT5(E444Q), or wildtype PRMT5(WT) in cardiac fibroblasts. As shown in Fig. 5c, overexpression of PRMT5(WT), but not PRMT5(E444Q), enhanced the levels of p-Smad3 and me-Smad3 in TGF-β1-stimulated cardiac fibroblasts. These data suggest that PRMT5 promotes TGF-β1-induced Smad3 phosphorylation through methylation modification.

Then, we confirmed the role of PRMT5 in cardiac fibroblast activation by inhibiting PRMT5 methyltransferase activity. As shown in Fig. 6a, overexpression of PRMT5(WT), but not PRMT5(E444Q) strengthened TGF-β1-induced expression of α-SMA and fibronectin in cardiac fibroblasts. A Smad3 inhibition rescue experiment with a

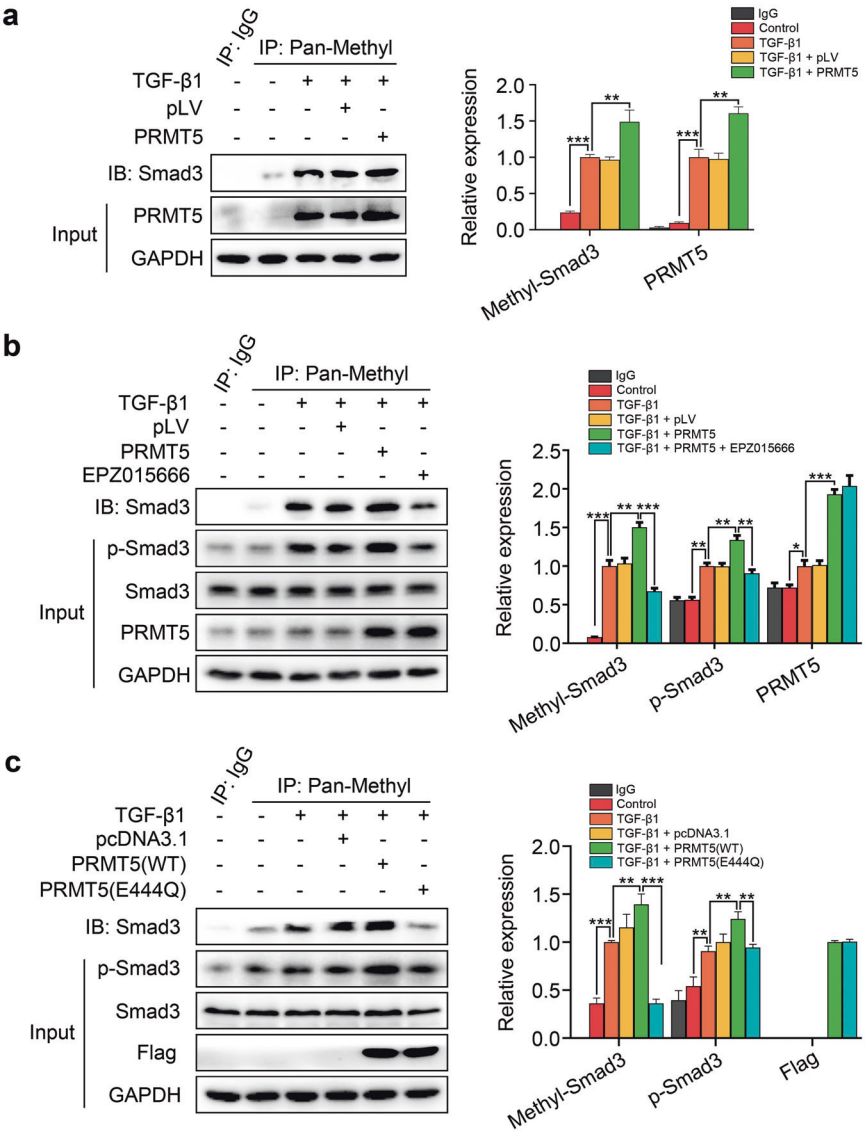

Fig. 5 PRMT5 promotes Smad3 phosphorylation through its methyltransferase activity. a Cardiac fibroblast transfected with pLV or PRMT5 plasmids were treated with TGF-β1 (5 ng/mL) for 24 h followed by immunoprecipitation with anti-Pan-Methyl antibody. The precipitates were analyzed by immunoblotting with indicating antibodies. **b** Cardiac fibroblasts transfected with pLV or PRMT5 plasmids were pre-treated with EPZ015666 (5 nM) and then with TGF-β1 (5 ng/mL) for 24 h followed by immunoprecipitation with anti-Pan-Methyl antibody. The precipitates were analyzed by immunoblotting with indicating antibodies. **c** Cardiac fibroblasts transfected with pcDNA3.1, PRMT5(WT) or PRMT5(E444Q) plasmids were treated with TGF-β1 (5 ng/mL) for 24 h followed by immunoprecipitation with anti-Pan-Methyl antibody. The precipitates were analyzed by immunoblotting with indicating antibodies. Data of at least three independent experiments are presented as mean ± SEM, $n = 6$, $^{*}P < 0.05$; $^{**}P < 0.01$; $^{***}P < 0.001$, compared with control.

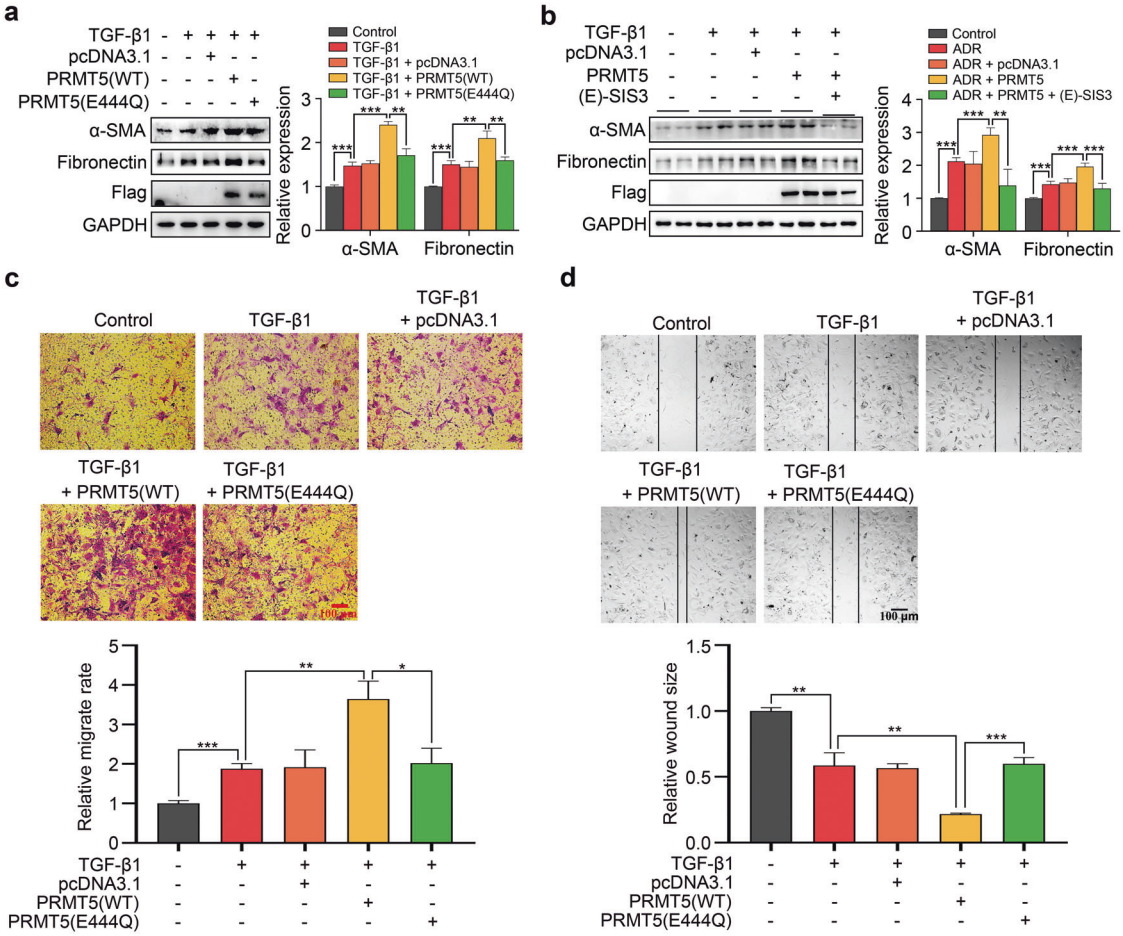

Fig. 6 PRMT5 promotes TGF-β1-mediated cardiac fibroblast activation dependent on its methyltransferase activity. a Cardiac fibroblast transfected with pcDNA3.1, PRMT5(WT) or PRMT5(E444Q) plasmids were treated with TGF-β1 (5 ng/mL) for 24 h followed by immunoblotting with indicated antibodies. **b** Cardiac fibroblasts transfected with pcDNA3.1 or PRMT5 plasmids were pre-treated with (E)-SIS3 and then treated with TGF-β1 (5 ng/mL) for 24 h followed by immunoblotting with indicated antibodies. **c**, **d** Cardiac fibroblasts transfected with pcDNA3.1, PRMT5(WT), or PRMT5(E444Q) plasmids were treated with TGF-β1 (5 ng/mL) for 24 h. Migration of cardiac fibroblasts was detected using transwell (**c**) and wound healing assay (**d**). Data of at least three independent experiments performed in duplicates are presented as mean ± SEM, $n = 6$, $^{*}P < 0.05$; $^{**}P < 0.01$; $^{***}P < 0.001$, compared with control.

Smad3 inhibitor (E)-SIS3 also showed that PRMT5 activated cardiac fibroblasts depending on Smad3 (Fig. 6b). Next, consistent with the effects on upregulation of α-SMA and fibronectin, overexpression of PRMT5(WT), but not PRMT5(E444Q) significantly promoted cardiac fibroblasts migration (Fig. 6c, d). Collectively, these results indicate that PRMT5 promotes Smad3 phosphorylation to activate cardiac fibroblast via methylation modification.

ADR-mediated PRMT5 upregulation was dependent on TGF-β1 autocrine

Since the above results showed PRMT5 was upregulated during ADR treatment, and given that TGF-β1 is a central cytokine involved in fibroblast activation [27], we then investigated whether ADR-induced PRMT5 expression in cardiac fibroblasts was dependent on TGF-β1. As shown in Fig. 7a, b, SB525334 abolished both ADR- and TGF-β1-induced PRMT5 upregulation (Fig. 7a) and subsequent cardiac fibroblast activation, evidenced by the reduction of α-SMA, and fibronectin (Fig. 7b). Consistent with the results in vivo, upregulation of PRMT5 was co-localized with α-SMA-positive activated cardiac fibroblasts induced by TGF-β1, which was abolished by SB525334 pretreatment (Fig. 7c). These results indicate that ADR induces PRMT5 expression and cardiac fibroblast activation depending on TGF-β1 autocrine.

DISCUSSION

In the present study, we identified the role of PRMT5 in ADR-induced cardiac fibrosis. Our results demonstrate that ADR induces PRMT5 upregulation, which critically mediates fibroblast activation and cardiac fibrosis. Mechanistically, PRMT5 overexpression promotes cardiac fibroblast activation by enhancing Smad3 phosphorylation, which is an effect depending on its methyltransferase activity (Fig. 8). Accordingly, our data support that PRMT5 is a novel mediator of cardiac fibrosis in ADR-induced cardiotoxicity.

Recently, it has been demonstrated that ADR can induce the expression and differentiation of TGF-β in cardiac fibroblasts [28]. ADR-induced TGF-β1 production by cardiac fibroblasts is known to widen its own expression in an autocrine manner, promoting the activation of cardiac fibroblasts [29]. Accordantly, in our research, we also discovered that TGF-β1 was boosted in vivo and in vitro after ADR treatment. Interestingly, the TGF-β receptor I inhibitor blocked the effect of ADR on activating cardiac fibroblasts, confirming that there is indeed a positive feedback regulation for TGF-β1 expression in ADR-stimulated cardiac fibroblasts.

Cardiac fibrosis is characterized by the induction of profibrotic growth factors, such as TGF-β1, and by the differentiation of cardiac fibroblasts into myofibroblasts. The fibrotic process is driven primarily by local myocardial increase in TGF-β1 [25]. In addition, studies have demonstrated that the expression of

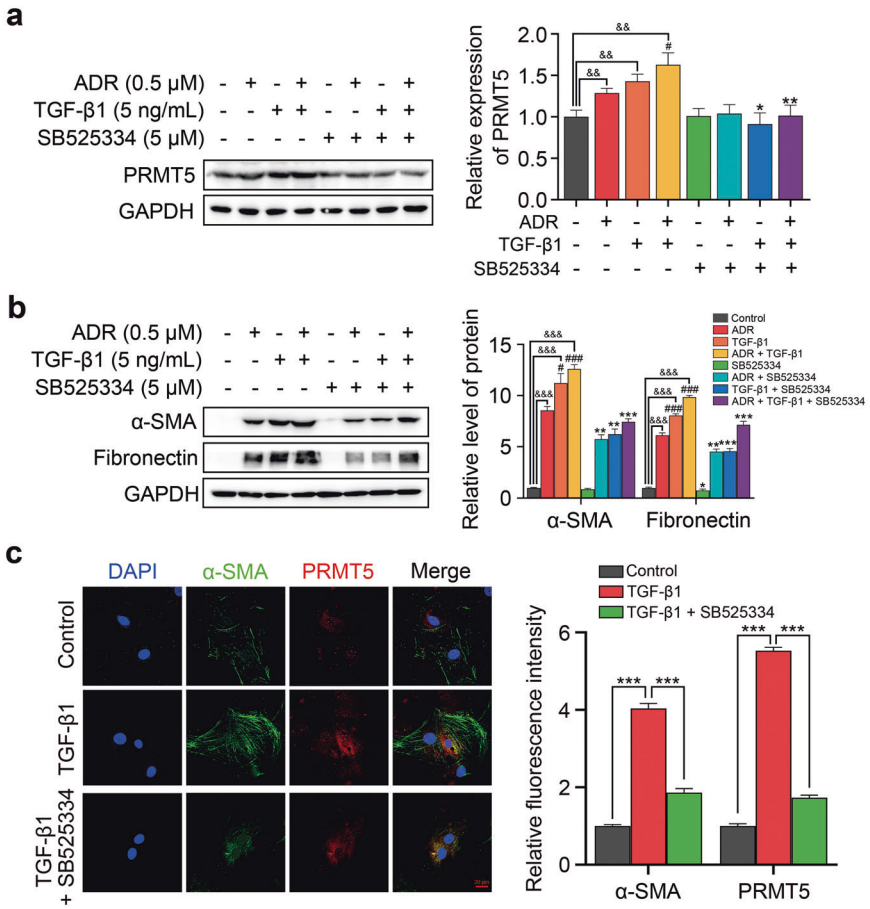

Fig. 7 ADR-induced PRMT5 expression in cardiac fibroblasts was dependent on TGF-β1. a Fibroblasts pre-incubated with SB525334 for 2 h were treated with ADR or TGF-β1 for 24 h, and then the cell lysates were subjected into immunoblotting with indicated antibodies. **b** Fibroblasts pre-incubated with SB525334 for 2 h were treated with ADR or TGF-β1 for 24 h, and then the cell lysates were subjected into immunoblotting with indicated antibodies. **c** Fibroblasts pre-incubated with SB525334 for 2 h were treated with TGF-β1 for 24 h, and then the cells were subjected into immunofluorescent staining and detected by the laser scanning confocal microscopy. Data of at least three independent experiments are presented as mean ± SEM, $n = 5$, $^{*}P < 0.05$; $^{**}P < 0.01$; $^{***}P < 0.001$, compared with control; $^{\#}P < 0.05$; $^{\#\#\#}P < 0.001$, compared with ADR-treated group; $^{\&\&}P < 0.01$; $^{\&\&\&}P < 0.001$, compared with non-treated group.

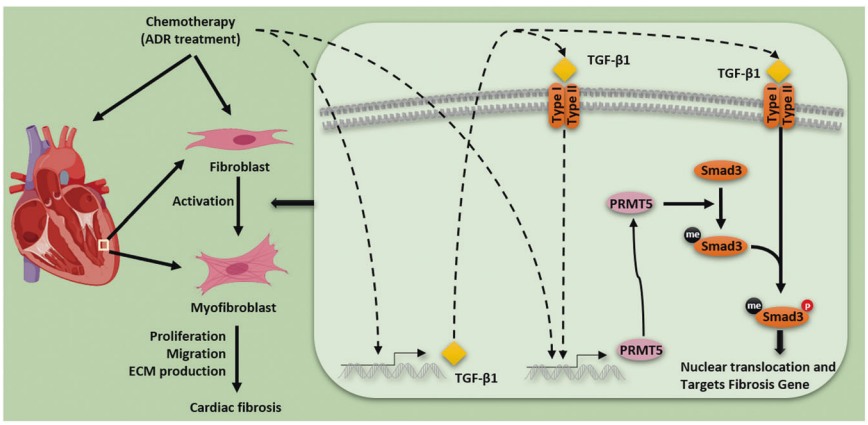

Fig. 8 Schematic representation of PRMT5 accelerating TGF-β1-induced fibroblasts activation via methylating Smad3 and promoting ADR-induced cardiac fibrosis. After ADR treatment, PRMT5 expression and TGF-β1 autocrine in cardiac fibroblasts were enhanced. On the one hand, autocrine TGF-β1 activates Smad3 to promote the expression of fibrosis genes, and also promotes PRMT5 expression; on the other hand, upregulated PRMT5 can stabilize Smad3 phosphorylation and ultimately promote fibrosis through methylation of Smad3.

TGF-β1 was boosted in the heart treated with ADR [30–33]. TGF-β1 acts to stimulate cardiac fibroblastic hyperplasia, increase the production of type I and III collagen, fibronectin and CTGF, and reduce collagen enzyme release to increase extracellular matrix accumulation [34–36]. Consistent with these findings, our results demonstrated that cardiac collagen I, fibronectin, and CTGF production markedly increased in ADR-treated mice, as similarly observed in TGF-β1-stimulated cardiac fibroblasts.

An intriguing finding in our study is that Smad3 maintains its own phosphorylation through PRMT5-mediated methylation. Mounting evidence has shown that posttranslational modifications (PTMs) of proteins have been implicated in the dynamic alterations of protein functions, and the crosstalk between these modifications makes PTMs notably vital for many biological processes [37–41]. Protein methylation, along with phosphorylation, regulates a variety of cellular functions through regulation of signaling pathways or gene expression [42–45]. Notably, it is reported that epidermal growth factor receptor (EGFR) methylation positively interacts with its phosphorylation, resulting in the alteration of EGFR activities [46]. A recent study has shown that PRMT1-mediated PLT3 arginine methylation at the 972/973 sites positively coordinates its phosphorylation at the Y696 site [47]. Sry-related HMG box 2 (Sox2), a known key stem cell-related factor, is capable of being both methylated and phosphorylated, and a switch between the two PTMs determines Sox2 stability and functions [26]. Previously, the interplay of phosphorylation and PTMs, such as ubiquitylation, has been demonstrated to coordinate Smad3 activation [48, 49]. Nonetheless, whether there exists a crosstalk between phosphorylation and methylation of Smad3 was not shown. In this study, we observed that Smad3 could be modified both by phosphorylation and methylation. Moreover, there exists a positive crosstalk between phosphorylation and PRMT5-mediated methylation of Smad3, which strengthens its activities in cardiac fibrosis. Nevertheless, it remains to be demonstrated whether Smad3 can be modified by other PTM crosstalk, or whether PRMT5 can affect the PTMs of other proteins through methylation or even play a role in other PTM forms. Hence, there is still much work to be done to thoroughly elucidate modulatory mechanisms of Smad3 and PRMT5 in cardiac fibrosis.

In summary, the present study indicates that PRMT5 acts as a profibrotic mediator in cardiac fibrosis. PRMT5 methylates Smad3 to reinforce its phosphorylation induced by TGF-β1, thus promoting cardiac fibrosis. Consequently, the current study supports PRMT5 as a promising therapeutic target for the treatment of cardiac fibrotic disease.

ACKNOWLEDGEMENTS

This work was financially supported by grants from the National Natural Science Foundation of China (Grant nos: 81973322, 81902706), Collaborative Innovation Center of Food Safety and Quality Control in Jiangsu Province, the Fundamental Research Funds for the Central Universities (Grant nos: JUSRP221037, JUSRP22007, JUSRP122055), Jiangsu Province "Six Summit Talents" Program (Grant no: YY-038) and Wuxi Taihu Talent Project.

AUTHOR CONTRIBUTIONS

LLP and JS designed the study and revised the paper. XLD, SZY, BHY, and HL performed experiments. XLD and XHP analysed the data. XLD wrote the paper. LLP and JS reviewed the paper.

ADDITIONAL INFORMATION

Supplementary information The online version contains supplementary material available at https://doi.org/10.1038/s41401-022-00963-x.

Competing interests: The authors declare no competing interests.

REFERENCES

1. Carvalho FS, Burgeiro A, Garcia R, Moreno AJ, Carvalho RA, Oliveira PJ. Doxorubicin-induced cardiotoxicity: from bioenergetic failure and cell death to cardiomyopathy. Med Res Rev. 2014;34:106–35.
2. Liu J, Cai Q, Wang W, Lu M, Liu J, Zhou F, et al. Ginsenoside Rh2 pretreatment and withdrawal reactivated the pentose phosphate pathway to ameliorate intracellular redox disturbance and promoted intratumoral penetration of adriamycin. Redox Biol. 2020;32:101452.
3. Anninga JK, Gelderblom H, Fiocco M, Kroep JR, Taminiau AHM, Hogendoorn PCW, et al. Chemotherapeutic adjuvant treatment for osteosarcoma: where do we stand? Eur J Cancer. 2011;47:2431–45.
4. Navarro-Hortal MD, Varela-Lopez A, Romero-Marquez JM, Rivas-Garcia L, Speranza L, Battino M, et al. Role of flavonoids against adriamycin toxicity. Food Chem Toxicol. 2020;146:111820.
5. Lother A, Bergemann S, Kowalski J, Huck M, Gilsbach R, Bode C, et al. Inhibition of the cardiacmyocyte mineralocorticoid receptor ameliorates doxorubicin-induced cardiotoxicity. Cardiovasc Res. 2018;114:282–90.
6. Zhang Y-W, Shi J, Li Y-J, Wei L. Cardiomyocyte death in doxorubicin-induced cardiotoxicity. Arch Immunol Ther Exp. 2009;57:435–45.
7. Takemura G, Fujiwara H. Doxorubicin-induccd cardiomyopathy from the cardiotoxic mechanisms to management. Prog Cardiovasc Dis. 2007;49:330–52.
8. Frangogiannis NG. Cardiac fibrosis. Cardiovasc Res. 2021;117:1450–88.
9. Varricchi G, Ameri P, Cadeddu C, Ghigo A, Madonna R, Marone G, et al. Antineoplastic drug-induced cardiotoxicity: a redox perspective. Front Physiol. 2018;9:167.
10. Medina-Gomez C, Bolanos J, Borbolla-Vazquez J, Munguia-Robledo S, Orozco E, Rodriguez MA. The atypical protein arginine methyltrasferase of Entamoeba histolytica (EhPRMTA) is involved in cell proliferation, heat shock response and in vitro virulence. Exp Parasitol. 2021;222:108077.
11. Liu M-Y, Hua W-K, Chen C-J, Lin W-J. The MKK-dependent phosphorylation of p38 alpha is augmented by arginine methylation on Arg49/Arg149 during erythroid differentiation. Int J Mol Sci. 2020;21:3546.
12. Zhu J, Zhang D, Liu X, Yu G, Cai X, Xu C, et al. Zebrafish prmt5 arginine methyltransferase is essential for germ cell development. Development. 2019;146:dev179572.
13. Stopa N, Krebs JE, Shechter D. The PRMT5 arginine methyltransferase: many roles in development, cancer and beyond. Cell Mol Life Sci. 2015;72:2041–59.
14. Kim H, Ronai ZeA. PRMT5 function and targeting in cancer. Cell Stress. 2020;4:199–215.
15. Calabretta S, Vogel G, Yu Z, Choquet K, Darbelli L, Nicholson TB, et al. Loss of PRMT5 promotes PDGFR alpha degradation during oligodendrocyte differentiation and myelination. Dev Cell. 2018;46:426–40.
16. Kota SK, Roening C, Patel N, Kota SB, Baron R. PRMT5 inhibition promotes osteogenic differentiation of mesenchymal stromal cells and represses basal interferon stimulated gene expression. Bone. 2018;117:37–46.
17. Liu Z, Ramachandran J, Vokes SA, Gray RS. Regulation of terminal hypertrophic chondrocyte differentiation in Prmt5 mutant mice modeling infantile idiopathic scoliosis. Dis Model Mech. 2019;12:dmm041251.
18. Kutner RH, Zhang XY, Reiser J. Production, concentration and titration of pseudotyped HIV-1-based lentiviral vectors. Nat Protoc. 2009;4:495–505.
19. Du M, Huang K, Huang D, Yang L, Gao L, Wang X, et al. Renalase is a novel target gene of hypoxia-inducible factor-1 in protection against cardiac ischaemia-reperfusion injury. Cardiovasc Res. 2015;105:182–91.
20. da Silva AR, Neri EA, Turaca LT, Dariolli R, Fonseca-Alaniz MH, Santos-Miranda A, et al. NOTCH1 is critical for fibroblast-mediated induction of cardiomyocyte specialization into ventricular conduction system-like cells in vitro. Sci Rep. 2020;10:16163.
21. Dong X, Yang Y, Zhou Y, Bi X, Zhao N, Zhang Z, et al. Glutathione S-transferases P1 protects breast cancer cell from adriamycin-induced cell death through promoting autophagy. Cell Death Differ. 2019;26:2086–99.
22. Chen X, Tong G, Fan J, Shen Y, Wang N, Gong W, et al. FGF21 promotes migration and differentiation of epidermal cells during wound healing via SIRT1-dependent autophagy. Br J Pharmacol. 2021;179:1102–21.
23. Guo W, Qiu W, Ao X, Li W, He X, Ao L, et al. Low-concentration DMSO accelerates skin wound healing by Akt/mTOR-mediated cell proliferation and migration in diabetic mice. Br J Pharmacol. 2020;177:3327–41.
24. Tallquist MD, Molkentin JD. Redefining the identity of cardiac fibroblasts. Nat Rev Cardiol. 2017;14:484–91.
25. Khalil H, Kanisicak O, Prasad V, Correll RN, Fu X, Schips T, et al. Fibroblast-specific TGF-beta-Smad2/3 signaling underlies cardiac fibrosis. J Clin Invest. 2017;127:3770–83.
26. Fang L, Zhang L, Wei W, Jin X, Wang P, Tong Y, et al. A methylation-phosphorylation switch determines Sox2 stability and function in ESC maintenance or differentiation. Mol Cell. 2014;55:537–51.
27. Stempien-Otero A, Kim DH, Davis J. Molecular networks underlying myofibroblast fate and fibrosis. J Mol Cell Cardiol. 2016;97:153–61.
28. Narikawa M, Umemura M, Tanaka R, Hikichi M, Nagasako A, Fujita T, et al. Doxorubicin induces trans-differentiation and MMP1 expression in cardiac fibroblasts via cell death-independent pathways. PLoS ONE. 2019;14:e0221940.
29. Pardoux C, Derynck R. JNK regulates expression and autocrine signaling of TGF-beta1. Mol Cell. 2004;15:170–1.
30. Tian X-Q, Ni X-W, Xu H-L, Zheng L, ZhuGe D-L, Chen B, et al. Prevention of doxorubicin-induced cardiomyopathy using targeted MaFGF mediated by nanoparticles combined with ultrasound-targeted MB destruction. Int J Nanomed. 2017;12:7103–19.

31. El-Said NT, Mohamed EA, Taha RA. Irbesartan suppresses cardiac toxicity induced by doxorubicin via regulating the p38-MAPK/NF-kappa B and TGF-beta 1 pathways. Naunyn Schmiedebergs Arch Pharmacol. 2019;392:647–58.
32. Sun Z, Lu W, Lin N, Lin H, Zhang J, Ni T, et al. Dihydromyricetin alleviates doxorubicin-induced cardiotoxicity by inhibiting NLRP3 inflammasome through activation of SIRT1. Biochem Pharmacol. 2020;175:113888.
33. Xu S, Wang Y, Yu M, Wang D, Liang Y, Chen Y, et al. LongShengZhi capsule inhibits doxorubicin-induced heart failure by antioxidative stress. Biomed Pharmacother. 2020;123:109803.
34. Sun X, Chen G, Xie Y, Jiang D, Han J, Chen F, et al. Qiliqiangxin improves cardiac function and attenuates cardiac remodelling in doxorubicin-induced heart failure rats. Pharm Biol. 2020;58:417–26.
35. Wang BQ, Hao JM, Jones SC, Yee MS, Roth JC, Dixon IMC. Decreased Smad 7 expression contributes to cardiac fibrosis in the infarcted rat heart. Am J Physiol Heart Circ Physiol. 2002;282:H1685–96.
36. Szabo Z, Magga J, Alakoski T, Ulvila J, Piuhola J, Vainio L, et al. Connective tissue growth factor inhibition attenuates left ventricular remodeling and dysfunction in pressure overload-induced heart failure. Hypertension. 2014;63:1235–40.
37. Zamaraev AV, Kopeina GS, Prokhorova EA, Zhivotovsky B, Lavrik IN. Post-translational modification of caspases: the other side of apoptosis regulation. Trends Cell Biol. 2017;27:322–39.
38. Deribe YL, Pawson T, Dikic I. Post-translational modifications in signal integration. Nat Struct Mol Biol. 2010;17:666–72.
39. Guo J, Dai X, Laurent B, Zheng N, Gan W, Zhang J, et al. AKT methylation by SETDB1 promotes AKT kinase activity and oncogenic functions. Nat Cell Biol. 2019;21:226–37.
40. Wang G, Long J, Gao Y, Zhang W, Han F, Xu C, et al. SETDB1-mediated methylation of Akt promotes its K63-linked ubiquitination and activation leading to tumorigenesis. Nat Cell Biol. 2019;21:214–25.
41. Li W, Wang HY, Zhao X, Duan H, Cheng B, Liu Y, et al. A methylation-phosphorylation switch determines Plk1 kinase activity and function in DNA damage repair. Sci Adv. 2019;5:eaau7566.
42. Nicholson TB, Chen T, Richard S. The physiological and pathophysiological role of PRMT1-mediated protein arginine methylation. Pharmacol Res. 2009;60:466–74.
43. Bedford MT, Clarke SG. Protein arginine methylation in mammals: who, what, and why. Mol Cell. 2009;33:1–13.
44. Biggar KK, Li SSC. Non-histone protein methylation as a regulator of cellular signalling and function. Nat Rev Mol Cell Biol. 2015;16:5–17.
45. Wei H, Mundade R, Lange KC, Lu T. Protein arginine methylation of non-histone proteins and its role in diseases. Cell Cycle. 2014;13:32–41.
46. Hsu JM, Chen CT, Chou CK, Kuo HP, Li LY, Lin CY, et al. Crosstalk between Arg 1175 methylation and Tyr 1173 phosphorylation negatively modulates EGFR-mediated ERK activation. Nat Cell Biol. 2011;13:174–81.
47. He X, Zhu Y, Lin Y-C, Li M, Du J, Dong H, et al. PRMT1-mediated FLT3 arginine methylation promotes maintenance of FLT3-ITD+ acute myeloid leukemia. Blood. 2019;134:548–60.
48. Guo X, Waddell DS, Wang W, Wang Z, Liberati NT, Yong S, et al. Ligand-dependent ubiquitination of Smad3 is regulated by casein kinase 1 gamma 2, an inhibitor of TGF-beta signaling. Oncogene. 2008;27:7235–47.
49. Guo X, Ramirez A, Waddell DS, Li Z, Liu X, Wang XF. Axin and GSK3- control Smad3 protein stability and modulate TGF- signaling. Genes Dev. 2008;22:106–20.